

人造沸石对甘薯不同链长直支链淀粉的分离效果

郭俊杰¹, 杨璐¹, 符芳芳¹, 连喜军^{1*}, 王雪青¹, 康海岐²

(1. 天津商业大学生物技术与食品科学学院, 天津市食品生物技术重点实验室, 天津 300134;

2. 四川省农业科学院作物研究所, 成都 610066)

摘要:柱层析法是根据混合物中各组分的理化性质差异,利用混合物中各组分在固定相和流动相中分配系数不同,经过多次分配将组分分离纯化。该文采用回生法分离甘薯直、支链淀粉后再进行二次回生,以窄化其分子链长,并采用柱层析法分离出不同分子量分布范围的淀粉组分,直、支链淀粉组分总制备率均大于2.4%。可见光谱及分子量分布研究表明,粒径为1~3 mm的人造沸石适合分离支链淀粉,粒径为4~6 mm的人造沸石适合分离直链淀粉。经大沸石分离,聚合度大的直链淀粉分子依赖沸石表面吸附,洗脱速度快,先被洗脱下来,聚合度较小的直链淀粉分子进入沸石孔隙内部,吸附力大,后被洗脱下来;经小沸石分离,甘薯支链淀粉组分F1b中分子量小、均一度高的组分先被洗脱下来,F2b中分子量大、均一度低的组分先被洗脱下来,说明甘薯直、支链淀粉的分支度对淀粉组分的分离也有一定影响。X射线衍射表明,甘薯直链淀粉组分在18.9°、23.4°、27.2°、29.3°、32.3°、33.7°附近出现强衍射峰,甘薯支链淀粉组分在21.6°、22.9°、23.9°、26.5°、27.1°、29.3°、34.1°、35.8°、39.5°附近也出现明显的衍射峰,此时甘薯直、支链淀粉的分子量分布指数(PDI, polydispersity index)均接近1.0。人造沸石柱层析可制备出分子量分布范围极窄的甘薯直、支链淀粉,该类淀粉表现出类似金属盐的X射线衍射峰,可作为深入研究淀粉大分子空间结构变化的材料。显微图片显示直链淀粉是由多个线型分子聚集在一起,呈典型的“柳条”状,而支链淀粉呈典型的“树枝”状。该研究提供了一种大量制备分子量分布范围极窄的直、支链淀粉的简单、高效方法,为深入探索淀粉大分子聚集过程中的形态变化创造了有利条件。

关键词:酶; 淀粉; 沸石; 柱色谱; 分离

doi: 10.11975/j.issn.1002-6819.2019.19.038

中图分类号: TS231 文献标识码: A 文章编号: 1002-6819(2019)-19-0307-08

郭俊杰, 杨璐, 符芳芳, 连喜军, 王雪青, 康海岐. 人造沸石对甘薯不同链长直支链淀粉的分离效果[J]. 农业工程学报, 2019, 35(19): 307—314. doi:10.11975/j.issn.1002-6819.2019.19.038 <http://www.tcsae.org>

Guo Junjie, Yang Lu, Fu Fangfang, Lian Xijun, Wang Xueqing, Kang Haiqi. Separation effect of sweet potato amylose and amylopectin with different chain length by artificial zeolite[J]. Transactions of the Chinese Society of Agricultural Engineering(Transactions of the CSAE), 2019, 35(19) : 307—314. (in Chinese with English abstract)
doi: 10.11975 / j. issn. 1002-6819.2019.19.038 <http://www.tcsae.org>

0 引言

直链淀粉和支链淀粉是淀粉的两大主要组分。甘薯淀粉中直链淀粉含量在15.3%~28.8%之间,而支链淀粉含量在71.2%~84.7%之间^[1]。直、支链淀粉的比例和含量对淀粉的产品加工、物化特性等有着直接影响^[2-3]。抗性淀粉(抗酶解淀粉)是一种不被健康人体小肠吸收,但能在大肠中发酵降解的淀粉,这类淀粉不仅可以增加食品的耐泡性、耐煮性^[4],延长食品货架期^[5],还具有增强人

体的工作耐力^[6],抑制肥胖^[7],预防心脑血管疾病等生理作用^[8]。抗性淀粉主要通过回生法制备,而淀粉的回生不仅取决于其分子大小、分子链长,还取决于其分子量分布指数(PDI polydispersitigindex)。淀粉分子分布越均匀,其回生性越好^[9]。研究表明,只有特定链长(DP 12-22)的淀粉分子才可以产生晶核并回生^[10-11]。淀粉的双螺旋结构在回生阶段产生,特定链长淀粉组分的比例越高,且分子量分布范围越窄,淀粉的回生率越高^[12]。甘薯淀粉为天然的高分子,其直、支链淀粉的分子量约为 $5\times10^5\text{ g/mol}$ ^[13]和 $1.6\times10^6\text{ g/mol}$ ^[14],且分子量分布很宽^[15],采用回生酶解的方法可以切断其高分子链,降低分子量,并使分子量分布变窄,从而加速淀粉回生^[16]。淀粉在高压湿热后进行酶解,淀粉链断裂,分子量变小,并产生不同分子量分布的淀粉分子。将不同链长淀粉分子分离纯化,得到较小PDI的淀粉组分,对于控制淀粉回生具有重要的意义。

柱层析法是根据混合物中各组分的理化性质差异,利用混合物中各组分在固定相和流动相中分配系数不

收稿日期:2019-05-09 修订日期:2019-06-21

基金项目:国家自然科学基金项目(31571834;31871811);天津市自然科学基金(18JCYBJC89900, 18JCDZDJ98200);天津市科技重大专项与工程(一二三产业融合发展科技示范工程 18ZXYENC00080)天津市高等学校创新团队“农产品加工贮藏新技术及相关机理研究”(TD13-5087)资助

作者简介:郭俊杰,博士,副教授,主要从事食品化学的研究。Email:gjjie@tjcu.edu.com
※通信作者:连喜军,副教授,博士,研究方向:回生淀粉研究。

Email:lianliu2002@163.com



同,经多次分配将各组分分离而达到纯化的目的^[17]。柱层析所需设备简单,且分离得到的产品纯度极高^[18],该法不仅可对天然产物进行分离纯化,还可以广泛应用于制药、食品、化工等领域中^[19]。沸石是自然界中一种广泛分布的多孔型架状硅酸盐矿物^[20],其比表面积大,具有较高的吸附能力及较强的离子交换能力,可用于柱层析的固定相中^[21]。以沸石为固定相可以分离不同链长的淀粉,而目前该方面相关研究较少。本文通过分别对甘薯直、支链淀粉进行回生酶解,使分子量分布变窄,然后采用沸石作为固定相,进行柱层析法分离,得到相近PDI的淀粉组分,并对其进行可见光谱、高效体积排阻柱色谱、X-射线衍射及显微图谱分析,探索沸石对不同分子量分布淀粉的分离效果,得到其分离的具体条件,为甘薯淀粉分离工艺的选择提供了相关理论基础。

1 材料与方法

1.1 材料与仪器

甘薯原淀粉:市售;α高温淀粉酶、无水乙醇、氢氧化钾、正丁醇(分析纯)、盐酸(分析纯):天津市风船化学试剂有限公司、人造沸石(大沸石粒径4~6 mm,小沸石粒径1~3 mm):天津市光复精细化工研究所。

Lambda25紫外可见分光光度计,美国PerkinElmer公司;D/max-2500 X-射线衍射分析仪,日本理学公司;高效体积排阻柱色谱系统(high performance size exclusion column chromatography system, HPSEC),系统配有多角度激光光散射检测器(multi-angle laser light scattering detector, MALS),折光率检测器(refractive index detector, RI)。串联双柱(300 mm×7.5 mm, PL aquagel-OH MIXED, 8 μm 凝胶色谱柱, 英国什罗普郡 Polymer 有限公司);DAWN DSP-F型激光光度计,采用He-Ne激光($\lambda=623.8\text{ nm}$)为光源;K-5贯流分析池,美国怀雅特技术公司,美国圣塔芭芭拉;RID-10A型差示折光仪,日本岛津公司;0.4 μm 薄膜滤器,Membrane Solutions 有限责任公司;OLYMPUS IX71型光学显微镜,日本奥林巴斯公司。

1.2 试验方法

1.2.1 人造沸石的活化

将人造沸石置于坩埚中,放入马沸炉,活化3 h后取出(600℃),以除去沸石中的杂质。

1.2.2 甘薯直、支链淀粉的制备

参照文献[22~24]方法制备甘薯回生淀粉,分离甘薯直链和支链淀粉,并将得到的直、支链淀粉二次回生、酶解、洗涤,干燥后备用。

1.2.3 沸石对甘薯回生淀粉组分分离

在100 mL 4 mol/L的KOH溶液中加入1.2.2中制备的甘薯回生淀粉1.0 g,水浴加热溶解后离心,取上清液,得到回生淀粉溶液。将得到的回生淀粉溶液倾倒入层析柱中,并向2个不同层析柱(20 mm×200 mm)中分别加入活化好的人造大、小沸石2500 g,直至淀粉溶液没过沸石1~2 cm即可。待吸附完成后(10 min),打开开关将淀粉溶液放出。将200 mL 0.01%草酸溶液分别倒入装有吸

附过回生淀粉的大、小沸石层析柱中,进行洗脱,将收集到的洗脱液按照先后顺序平均分为4等份。取各洗脱液组分5 mL于试管中,分别滴加1滴碘液,静置30 min。观察碘液颜色,判断大、小沸石吸附直、支链淀粉的情况。

1.2.4 柱层析法分别分离甘薯直链、支链淀粉组分

在1 000 mL 4 mol/L的KOH溶液中加入1.2.2步骤制备的甘薯直、支链淀粉8 g,水浴加热溶解后离心,取上清液,得到直链和支链淀粉溶液。将得到的直、支链淀粉溶液分别倾倒入装有大、小沸石的层析柱(沸石质量2500 g)中,直至淀粉溶液没过沸石1~2 cm即可。吸附10 min后打开开关将淀粉溶液放出。将2000 mL 0.01%草酸溶液,分别倒入装有吸附过直、支链淀粉的沸石层析柱中,进行洗脱,将收集到的洗脱液平均分为4等份(留取中间的第二组份和第三组份)。将得到的直链淀粉组分记为F1a、F2a,支链淀粉组分记为F1b、F2b。

将F1a、F2a、F1b、F2b分别倒入4颗层析柱中,向层析柱中分别加入活化后的大沸石(F1a、F2a)和小沸石(F1b、F2b),直至直、支链淀粉溶液没过沸石1~2 cm。待吸附10 min后,将液体放出并弃去。再分别用2000 mL 0.01%草酸溶液洗脱4颗层析柱。将收集到的洗脱液分别平分为4等份:第一份回收,第二份至第四份分别编号,直链淀粉为F1a-1、F1a-2、F1a-3和F2a-1、F2a-2、F2a-3,支链淀粉为F1b-1、F1b-2、F1b-3和F2b-1、F2b-2、F2b-3。最后将分离得到的各淀粉组分减压蒸馏浓缩后,离心分离,沉淀充分水洗,干燥。

1.2.5 淀粉可见吸收测定

将分离得到的淀粉溶液用4 mol/L的盐酸调节pH值至7.0,再分别量取各组份溶液25 mL,加3滴碘液^[25],放置30 min后,用Lambda25紫外可见分光光度计测定可见吸收的最大吸收波长。

1.2.6 X-射线测定

用铜箔和镍箔包裹淀粉粉末采用X-射线衍射仪扫描,扫描电流和电压分别为27 mA和50 kV,扫描衍射角(2θ)从4°到40°,步长为0.05,间隔时间为2 s。

1.2.7 分子量分布曲线

如文献[26]所述,将100 g样品加到80 mL去离子水中,然后在沸水中加热并搅拌20 min使样品完全溶解。通过5 μm的醋酸纤维素滤膜过滤后,将溶解后的样品放入高效体积排阻柱色谱系统中。流动相速度为0.5 mL/min。流动相为含0.02%NaN₃的0.1 mol/L NaNO₃溶液,该溶液通过0.4 μm薄膜滤器过滤。分子量计算时,比折光指数增量(dn/dc)值为0.150,数据处理采用ASTRA软件(4.73.04版)。

1.2.8 光学显微图

将制备的淀粉样品片置于显微镜样品台上,观察淀粉颗粒的形貌。在B光(波长420~480 nm)下对淀粉颗粒进行拍照。

2 结果与讨论

2.1 大小人造沸石分离甘薯回生淀粉

图1为淀粉经小沸石和大沸石洗脱后淀粉组分加碘

液的显色反应。

由图1a可知,人造小沸石洗脱下来的组分基本呈现粉红色,说明小沸石吸附的主要分支链淀粉。由图1b可知,人造大沸石的3、4组分呈现深蓝色,说明大沸石可吸附大量直链淀粉,而且洗脱过程中支链淀粉先洗下来,直链淀粉后洗下来。因此,后续试验用人大沸石分离直链淀粉组分,人造小沸石分离支链淀粉组分。



图1 经沸石洗脱后淀粉各组分加碘液的显色反应(洗脱先后顺序为1,2,3,4)

Fig.1 Chromogenic reactions of starch components separated by zeolite

2.2 采用人造沸石分离直、支链淀粉

表1为以大、小沸石为固定相,采用柱层析法,分别分离100 g甘薯直、支链淀粉得到的各组分的质量。并按下式计算得到直、支链淀粉的制备率。

表1 采用人造沸石分离的甘薯直、支链淀粉各组分质量
(100 g干淀粉)

Table 1 Weight of sweet potato amylose and amylopectin separated by artificial zeolite (100 g dry starch)

样品 Sample	编号 No.	产量 Yield/(mg)
直链淀粉 Amylose	F1a-1	488
	F1a-2	474
	F1a-3	487
	F2a-1	464
	F2a-2	461
	F2a-3	426
支链淀粉 Amylopectin	F1b-1	427
	F1b-2	414
	F1b-3	413
	F2b-1	409
	F2b-2	399
	F2a-3	388

$$\text{制备率}(\%) = \frac{\sum m_i}{100} \times 100\% \quad (1)$$

式中 m_i 为 100 g 直链或支链淀粉分离得到的不同组分淀粉的质量。直链淀粉各组分质量在 450 mg 左右,100 g 甘薯直链淀粉经柱层析分离得到各组分总质量为 2800 mg, 制备率高达 2.8%。支链淀粉各组分质量在 410 mg 左右,100 g 甘薯支链淀粉经柱层析分离得到各组分总质量为 2450 mg, 制备率为 2.45%, 远远高于普通液相制备色谱对有机分子的分离^[27]。

2.3 可见吸收测定

碘分子可嵌入淀粉的双螺旋结构内部而生成蓝紫色络合物^[28-29], Gidley 和 Bulpin 等的研究表明^[30], 只有聚合

度大于 10 的淀粉才能形成双螺旋结构。由图 2a、2b 可知, 经人造大沸石分离直链淀粉得到的组分加碘液后, 除了 F1a-1 有 558 nm 最大吸收外, 其他组分在可见光区没有发现明显的吸收, 表明其聚合度均小于 10, 双螺旋结构在分离过程中打开, 而后却没有重新形成。回生淀粉中直链淀粉组分聚合度大多小于 10, 说明直、支链淀粉混合回生过程中, 一个长直链淀粉链可以和很多个支链或直链淀粉形成氢键, 长直链淀粉有部分间隔的链段没有形成氢键, 该链段由于在淀粉酶水解过程中被水解而断裂成多个小的链段。由图 2c、2d 可知, 经人造小沸石分离支链淀粉所得组分加碘液后均出现了明显的可见吸收, 表明其分子聚合度均大于 10, 并且保持了双螺旋结构。洗脱后的甘薯支链淀粉组分的最大吸收波长为: $\lambda_{F1b-2} > \lambda_{F1b-1} > \lambda_{F2a-3} > \lambda_{F2b-1} > \lambda_{F2b-2} > \lambda_{F2b-3}$, 说明小沸石柱层析分离甘薯支链淀粉过程中聚合度大的组分先被分离出来, 聚合度小的后分离出来。大、小沸石分离甘薯直、支链淀粉均是聚合度大的组分先分离出来, 说明人造沸石孔径大于聚合度为 10 的淀粉分子直径, 所以聚合度较小的淀粉分子可进入沸石孔隙, 吸附力大, 后被洗脱下来; 而聚合度大的淀粉分子依赖沸石表面吸附, 洗脱速度快, 先被洗脱下来。

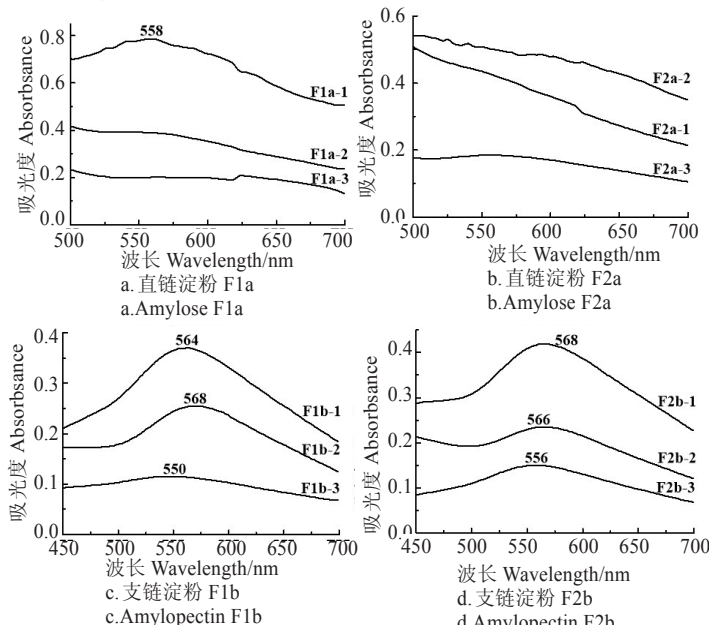


图2 甘薯直、支链淀粉的可见吸收光谱
Fig.2 Vis spectrum of sweet potato amylose and amylopectin components

2.4 人造沸石分离直、支链淀粉的分子量分布研究

图4、图5和表2为回生酶解后, 以大、小沸石为固定相采用柱层析法分离得到的甘薯直、支链淀粉各组分的分子量分布。文献报道^[30]抗性淀粉的均分子量(M_w)为 18 614 g/mol, 数均分子量(M_n)为 12 681 g/mol, 分子量分布指数(PDI)为 1.468, 分子量分布较宽。本试验结果表明, 通过回生酶解, 直链淀粉和支链淀粉的 M_w 分别变窄为 1 641~2 069 g/mol 和 1 671~2 167 g/mol, M_n 则变窄为 1 516~1 710 g/mol 和 1 526~1 678 g/mol。对应的直链淀粉 PDI 范围为 1.082~1.209, 支链淀粉 PDI 为 1.095~1.291, 说明通过酶解回生淀粉制备出的甘薯直、支链淀粉的分子量分布比回生淀粉本身的分子量分布范围要窄很多。

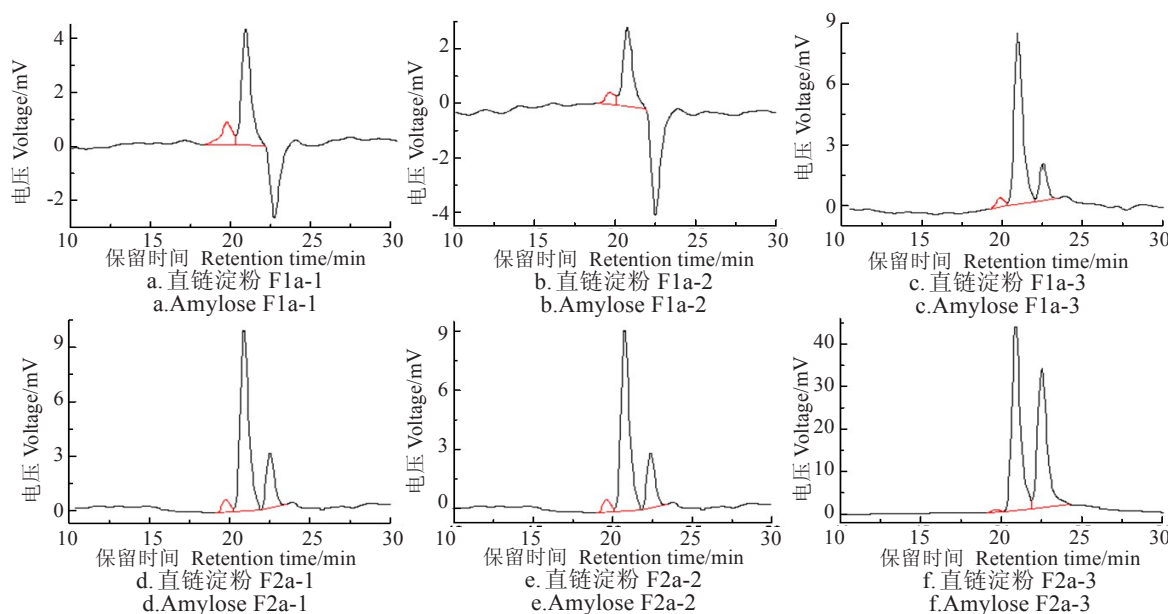


图3 甘薯直链淀粉的分子量分布图

Fig.3 Molecular weight distribution curve of sweet potato amylose

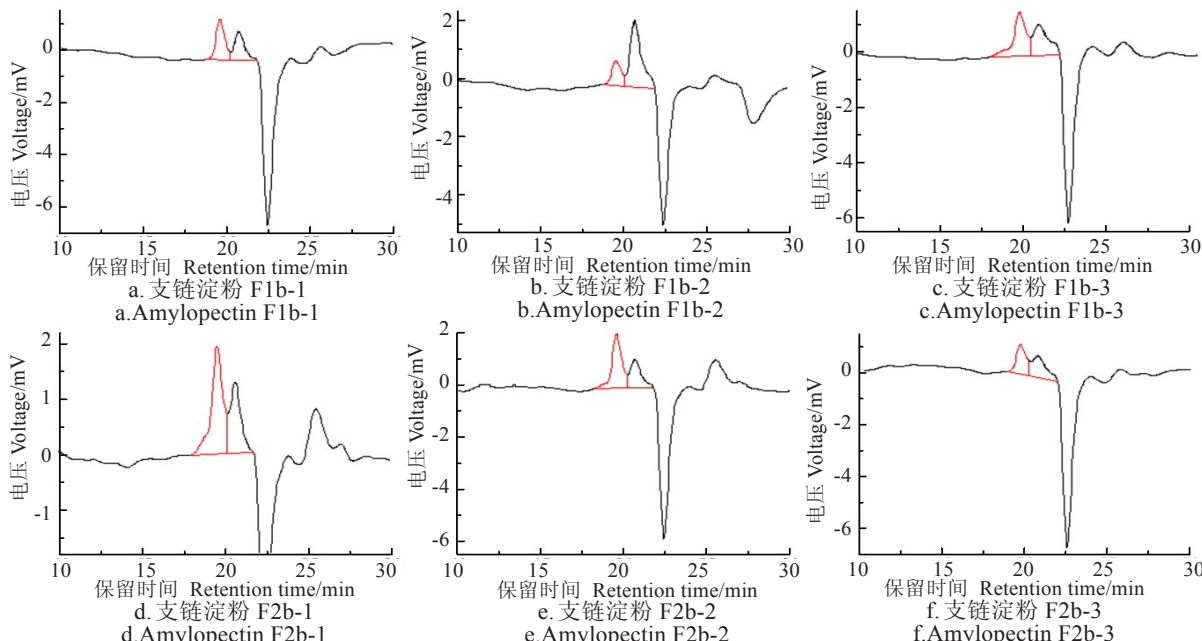


图4 甘薯支链淀粉的分子量分布图

Fig.4 Molecular weight distribution curve of sweet potato amylopectin

表2 甘薯淀粉的分子量分布

Table 2 Molecular weight distribution of sweet potato starch

样品 Sample	编号 No.	M_w	M_n	PDI ($\frac{M_w}{M_n}$)
直链淀粉 Amylose	F1a-1	2 069	1710	1.209
	F1a-2	1 641	1516	1.082
	F1a-3	1 692	1581	1.070
	F2a-1	1 692	1590	1.064
	F2a-2	1 645	1543	1.066
	F2a-3	1 759	1681	1.046
支链淀粉 Amylopectin	F1b-1	1 734	1586	1.093
	F1b-2	1 693	1549	1.093
	F1b-3	2 167	1659	1.306
	F2b-1	2 073	1678	1.235
	F2b-2	1 840	1599	1.150
	F2b-3	1 671	1526	1.095

注: M_w 为重均分子量, M_n 为平均分子量。Note: M_w is weight average molecular weight; M_n is number average molecular weight.

由表2、图3可知,甘薯直链淀粉组分F1a的1、2、3组分中的PDI分别为1.209、1.082和1.070,按照洗脱先

后顺序,组分的均一性越来越强。组分F1a-1的PDI明显高于组分F1a-2和F1a-3,推测F1a-1的直链淀粉未进入人造大沸石孔隙内,而是吸附于沸石表面。F2a所有组分的PDI均接近1.0,即重均和数均分子量接近,说明分子量非常均一。F2a的所有直链淀粉组分都进入了人造大沸石的孔隙内,进入大沸石孔隙内的甘薯直链淀粉经过大沸石柱层析,可制备出分子量分布范围极窄的直链淀粉。

由表2、图4可知,甘薯支链淀粉组分F1b的1、2、3组分中的PDI分别为1.093、1.093和1.306,1、2组分的均一度接近且高于组分3。组分F1b-3的PDI明显高于组分F1b-1和F1b-2,推测F1b-3的甘薯支链淀粉分子直径大于人造小沸石的孔径,没能进入小沸石孔隙,而是吸附于沸石表面。组分F1b-3最后洗脱下来是由于小沸石表面吸附该组分的吸附力大于小沸石孔隙内表面对组分F1b-1和F1b-2的吸附。按照洗脱顺序,甘薯支链淀粉F2b所

有组分的PDI值依次减小。最后洗脱下来的F2b-3的PDI最小。组分F2b-1和组分F1b-3的分子量虽然接近,但洗脱顺序不同,F2b-1先被洗脱,这可能与两种分子的分支度不同有关,后者分支度大,淀粉分子与小沸石吸附力更强,所以后被洗脱。甘薯支链淀粉组分F1b的整体分支度可能要比组分F2b的大。

2.5 X-射线衍射分析

由于组成淀粉的直链和支链淀粉晶体结构及比例不同,淀粉颗粒分为有序的结晶区和无序的无定形区两部分^[32]。直、支链淀粉的晶体特性(聚集状态)一般通过X-射线衍射法进行研究^[33]。A型结构淀粉在15°和23°附近具有较强的衍射峰,同时在17°和18°处出现双峰;B型结构在17°附近具有最强的衍射峰,同时在15°,20°,22°和24°处也有一些较小的衍射峰,其典型标志是5.6°的衍射峰;C型结构是A型和B型的混合物,在17°和23°附近出现强衍射峰,在5.6°和15°处出现一些弱峰,且干燥样品中5.6°处的衍射峰可能会消失。而V型结构的衍射峰出现在7.8°,13.5°和20.7°附近^[34-36]。

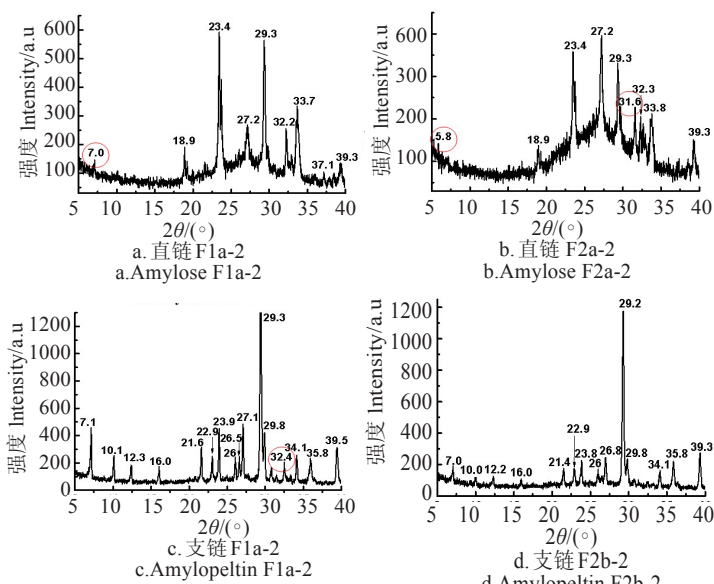


图5 甘薯直、支链淀粉组分的X射线衍射图谱

Fig.5 XRD spectrum of sweet potato amylose and amylopectin

图5为甘薯直、支链淀粉组分的X射线衍射图谱,由图可知,甘薯直链和支链淀粉组分呈现出类似金属盐晶体的X射线尖锐衍射峰,甘薯直链淀粉组分F1a-2(图5a)衍射角出现在7°、18.9°、23.4°、27.2°、29.3°、32.2°、33.7°、39.3°。甘薯直链淀粉组分F2a-2(图5b)衍射角出现在5.8°、18.9°、23.4°、27.2°、29.3°、31.6°、32.3°、33.7°、39.3°,这与文献报道^[37-38]分子量分布范围在3~6×10³ g/mol之间淀粉的X射线衍射峰不同,该类淀粉的衍射峰型一般较宽,且峰数较少,很少见锐利的尖峰。直链F2a-2比F1a-2的聚合度低,其衍射峰多了31.6°(对应面间距1.47 Å),另外弱峰7°衍射角变为5.8°,出现了晶体面间距较大的晶面,说明聚合度越低的直链淀粉越容易形成更多的晶面。甘薯支链淀粉组分F1b-2在7.1°、10.1°、12.3°、16.0°、21.6°、22.9°、23.9°、26.5°、27.1°、29.3°、32.4°、34.1°、35.8°、39.5°附近均出现了明显的衍射峰,而甘薯支链淀粉组分F2b-2在衍射角为7.0°、10.0°、12.2°、16.0°处衍射峰明显

减小,衍射角为32.4°(对应面间距1.43 Å)的晶面消失。甘薯支链淀粉组分F2b-2比组分F1b-2的聚合度低,但晶体衍射峰少,说明F2b-2中部分甘薯支链淀粉长度太小,不足以形成稳定的分子间氢键而产生晶面。分子量分布范围极窄的甘薯直、支链淀粉表现出类似金属盐的X射线衍射峰,可作为深入研究淀粉大分子空间结构变化的材料。

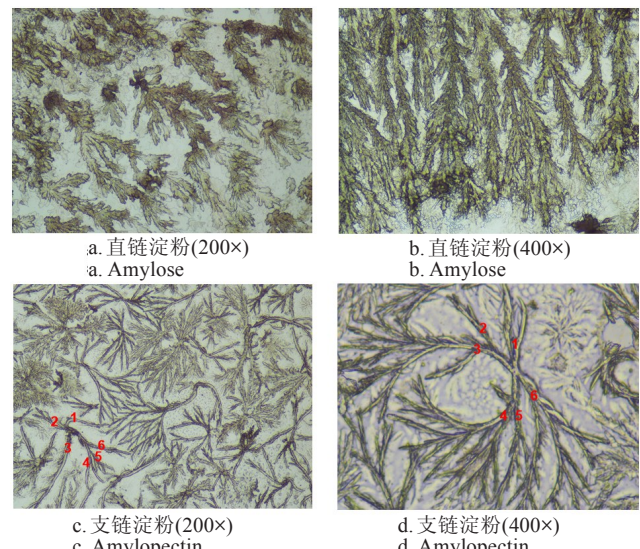


图6 甘薯淀粉光学显微图片
Fig.6 Optical micrograph of sweet potato amylose and amylopectin

2.6 显微图像分析

直链淀粉是一种线形多聚物,主要由α-D-1,4-糖苷键连接而成,还有一部分由α-D-1,6-糖苷键连接而成^[39-40]。淀粉在外加条件(热处理、溶剂处理等)的作用下,由于分子内氢键发生相互作用,使得直链淀粉的链状结构发生旋转,形成了容易与一些疏水基团发生内络合作用的左手螺旋空腔结构^[41]。由图6a,6b可见,甘薯直链淀粉是由多个线型分子聚合在一起,呈典型的“柳条”状,末端侧支较短,C链较长。

而支链淀粉是一种高分枝的束状聚合物,主链通过α-1,4-糖苷键连接而成,支链通过α-1,6-糖苷键与主链相连^[32]。甘薯支链淀粉光学显微图片(图6c,6d)显示支链淀粉呈典型的枝型“树枝”状,每个甘薯支链淀粉有6个发散的分支(图6c和图6d中数字标识处),这与前期研究结果吻合^[42],其“树枝”状结构中的分支并非均匀分布,而是分成小群体的分支群,可以通过α-淀粉酶彻底水解分离得到分支群,从而进一步降低分子质量,分离得到分子量分布更加均一度的淀粉组分。甘薯直、支链淀粉的显微结构与文献推测的淀粉直、支链微观结构类似^[43-46]。

3 结论

柱层析法可有效分离甘薯直、支链淀粉,研究表明粒径为1~3 mm的人造沸石适合分离支链淀粉,粒径为4~6 mm的人造沸石适合分离直链淀粉。通过回生、酶解、柱层析分离后,直链淀粉和支链淀粉的重均分子量分别变窄为1 641~2 069 g/mol和1 671~2 167 g/mol,甘

薯直、支链淀粉组分的分子直径及分支度均对沸石柱层析法分离不同链长的淀粉有着显著影响。当甘薯直、支链淀粉的PDI接近1.0时,直链淀粉组分在18.9°、23.4°、27.2°、29.3°、32.3°、33.7°附近,支链淀粉组分在21.6°、22.9°、23.9°、26.5°、27.1°、29.3°、34.1°、35.8°、39.5°附近均出现类似金属盐的X射线衍射强峰。甘薯直链淀粉呈典型的“柳条”状,而甘薯支链淀粉呈典型的枝型“树枝”状。其枝条状结构可以通过 α -淀粉酶彻底水解分离得到分支群,从而进一步降低分子质量,分离得到分子量分布更加均一度的淀粉组分。柱层析法有望得到大量分子量分布范围极窄的直、支链淀粉,该研究为探索淀粉大分子聚集过程中的形态变化创造了有利条件。

[参考文献]

- [1] Chen Z H. Physicochemical Properties of Sweet Potato Starches and Their Application in Noodle Products[D]. The Netherlands Wageningen University, 2003.
- [2] Xie F G, Yu L, Su Bing, et al. Rheological properties of starches with different amylose / amylopectin ratios[J]. Journal of Cereal Science, 2009, 49(3): 371—377.
- [3] Liu H S, Yu L, Simon G, et al. Effects of annealing on gelatinization and microstructures of corn starches with different amylose / amylopectin ratios[J]. Carbohydrate Polymers, 2009, 77(3): 662—669.
- [4] Birt D F, Boylston T, Hendrich S, et al. Resistant Starch: Promise for Improving Human Health[J]. Advances in Nutrition, 2013, 4 (6): 587—601.
- [5] Klosterbuer A S, Hullar M A J, Li F, et al. Gastrointestinal effects of resistant starch, soluble maize fiber and pullulan in healthy adults[J]. British Journal of Nutrition, 2013, 110(6): 1068—1074.
- [6] Hu X P, Xie Y Y, Jin Z Y, et al. Effect of single-, dual-, and triple-retrogradation treatments on in vitro digestibility and structural characteristics of waxy wheat starch[J]. Food Chemistry, 2014, 157: 373—379.
- [7] Polakof S, Diaz-Rubio M E, Dardevet D, et al. Resistant starch intake partly restores metabolic and inflammatory alterations in the liver of high-fat-diet-fed rats[J]. Journal of the Nutritional Biochemistry, 2013, 24 (11): 1920—1930.
- [8] Keenan M J, Zhou J, Hegsted M, et al. Role of resistant starch in improving gut health, adiposity, and insulin resistance[J]. Advances in Nutrition, 2015, 6(2): 198—205.
- [9] Chang Y H, Lin J H. Effects of molecular size and structure of amylopectin on the retrogradation thermal properties of waxy rice and waxy cornstarches[J]. Food Hydrocolloids, 2007, 21(4): 645—653.
- [10] Lian X, Dong S, Gao K, et al. Sweet potato amylose and amylopectin with narrower distribution of molar mass and chain length obtained by a repeated retrogradation - hydrolysis procedure[J]. Journal of Applied Polymer, 2016, 133(34): 8311—8319.
- [11] Vandepitte G E, Ermeylen R, Geeroms V J, et al. Rice starches. III. Structural aspects provide insight in amylopectin retrogradation properties and gel texture[J]. Journal of Cereal Science, 2003, 38(1): 61—68.
- [12] Lian X J, Kang H Q, Sun H B, et al. Identification of the main retrogradation-related properties of rice starch[J]. Journal of Agricultural and Food Chemistry, 2015, 63(5): 1562—1572.
- [13] Radosta S, Haberer M, Vorwerg W. Molecular characteristics of amylose and starch in dimethyl sulfoxide[J]. Biomacromolecules, 2001, 2(3): 970—978.
- [14] Tetchi F A, Rolland-Sabate A, Amani G N, et al. Molecular and physicochemical where science meets business characterisation of starches from yam, cocoyam, cassava, sweet potato and ginger produced in the Ivory Coast[J]. Journal of the Science of Food and Agriculture, 2007, 87(10): 1906—1916.
- [15] Wang K, Hasjim J, Wu A C, et al. Variation in amylose fine structure of starches from different botanical sources[J]. Journal of Agricultural and Food Chemistry, 2014, 62(19): 4443—4453.
- [16] Pfannemüller B. Influence of chain length of short monodisperse amyloses on the formation of A - and B-type X-ray diffraction patterns [J]. International Journal of Biological Macromolecules, 1987, 9(2): 105—108.
- [17] Rothstein F. A column design for reverse-flow sephadex gel permeation chromatography[J]. Journal of chromatography, 1965, 18 (1): 36—41.
- [18] Smith J D. Plastic chromatography columns[J]. Laboratory Practice, 1971, 2(6): 496.
- [19] Gunawan S, Ismadji S, Ju, Y H. Design and operation of a modified silica gel column chromatography[J]. Journal of the Chinese Institute of Chemical Engineers, 2008, 39(6): 625—633.
- [20] Wu Y Y, Yang C X, Yan X P. An in situ growth approach to the fabrication of zeolite imidazolate framework-90 bonded capillary column for gas chromatography separation[J]. Analyst, 2015, 140(9): 3107—3112.
- [21] Macko T, Pasch H, Denayer J F. Adsorption of polypropylene from dilute solutions on a zeolite column packing[J]. Journal of Separation Science, 2005, 28(1): 59—64.
- [22] Guo J J, Lian X J, Kang H Q, et al. Effects of glutenin in wheat gluten on retrogradation of wheat starch[J]. European Food Research and Technology, 2016, 242: 1485—1494.
- [23] Guo J J, Kang H Q, Feng X, et al. The interaction of sweet potato amylose / amylopectin and KCl during drying[J]. Food Hydrocolloids, 2014, 41: 325—331.
- [24] 郭俊杰, 孙海波, 李琳, 等. 参与回生玉米直链和支链淀粉理化特性[J]. 食品工业科技, 2014, 35(14): 91—94.
Guo Junjie, Sun Haibo, Li Lin, et al. Study on physicochemical characteristics of amylose and amylopectin fractions from retrograded maize starch[J]. Science and Technology of Food Industry, 2014, 35(14): 91—94. (in Chinese with English abstract)
- [25] Lian X J, Wang C J, Zhang K S, et al. The retrogradation properties of glutinous rice and buck wheat starches as observed with FT-IR, ^{13}C NMR and DSC[J]. International Journal of Biological Macromolecules, 2014, 64(3): 288—293.
- [26] Philpot K, Martin M, Butardo V, et al. Environmental factors that affect the ability of amylose to contribute to retrogradation in gels made from rice flour[J]. Journal of Agricultural and Food Chemistry, 2006, 54(14): 5182—5190.
- [27] Mario B. Aranda, Mario H. Vega, Ricardo F. Villegas, Routine Method for Quantification of Starch by Planar Chromatography (HPTLC), JPC-Journal of Planar Chromatography-Modern TLC [J]. 2005, 18(104): 285-289.
- [28] Chauhan F, Seetharaman K. On the organization of chains in amylopectin[J]. Starch, 2013, 64(3): 191—199.
- [29] Banks W, Greenwood, Khan K M. The interaction of linear, amy-

- lase oligomers with iodine[J]. Carbohydrate Polymer, 1971, 17(1): 25—33.
- [30] Gidley M. J; Bulpin, P V. Crystallisation of maltooligosaccharides as models of the crystalline forms of starch: Minimum chain-length requirement for the formation of double helices[J]. Carbohydrate Research, 1987, 161, 291—300.
- [31] 杨光, 丁霄霖. 抗性淀粉分子量分布的研究[J]. 中国粮油学报, 2000, 15(5): 37—40.
Yang Guang, Ding Xiaolin. Studies on molecular weight distribution of resistant starch[J]. Journal of the Chinese Cereals and Oils Association, 2000, 15(5): 37 — 40. (in Chinese with English abstract)
- [32] 李海普, 李彬, 欧阳明, 等. 直链淀粉和支链淀粉的表征[J]. 食品科学, 2010, 31(11): 273—277.
Li Haipu, Li Bin, Ouyang Ming, et al. Advances in characterization of amylose and amylopectin starch[J]. Food Science, 2010, 31 (11): 273—277. (in Chinese with English abstract)
- [33] Chen L, Ma R R, McClements D J, et al. Impact of granule size on microstructural changes and oil absorption of potato starch during frying[J]. Food Hydrocolloids, 2019, 94: 428—438.
- [34] Cheetham N W H, Tao L. Variation in crystalsline type with content in maize starch granules: an X-ray powder diffraction study [J]. Carbohydrate Polymer, 1998, 36(4), 277—284.
- [35] Christopher G O. Towards an understanding of starch granule structure and hydrolysis[J]. Trends in Food Science & Technology, 1997, 8(11): 375—382.
- [36] Lu X X, Luo Z G, Fu X, et al. Two-step method of enzymatic synthesis of starch laurate in ionic liquids[J]. Journal of Agricultural and Food Chemistry, 2013, 61(41), 9882—9891.
- [37] 郭俊杰, 马乔治, 康海岐, 等. 含醇溶蛋白小麦回生抗性直支链淀粉性质分析[J]. 农业工程学报, 2018, 34(4): 293—298.
Guo Junjie, Ma Qiaozhi, Kang Haiqi, et al. Property analysis of resistant wheat amylose and amylopectin with wheat gliadin starch [J]. Transactions of the Chinese Society for Agricultural Engineering (Transactions of the CSAE), 2018, 34(4): 293 — 298. (in Chinese with English abstract)
- [38] 孙冰华. 线性糊精的制备、相行为及应用[D]. 无锡: 江南大学, 2018.
Sun Binghua. Preparation, Phase Behavior and Application of Linear Dextrin[D]. Wuxi: Jiangnan University, 2018. (in Chinese with English abstract)
- [39] Yoshida H, Nozaki K, Hanashiro I. Structure and physicochemical properties of starches from kidney bean seeds at immature, premature and mature stages of development[J]. Carbohydrate Research, 2003, 338(5): 463—469.
- [40] Yoshimoto Y, Takenouchi T, Takeda Y. Molecular structure and some physicochemical properties of waxy and low-amylase barley starches[J]. Carbohydrate Polymers, 2002, 47(2): 159—167.
- [41] Lopez C A, Vries A H, Marrink S J. Amylose folding under the influence of lipids[J]. Carbohydrate Research, 2012, 364: 1—7.
- [42] Lian X J, Li L, Zhang K S, et al. A new proposed sweet potato starch granule structure-pomegranate concept[J]. International Journal of Biological Macromolecules. 2012, 50(3): 471—475.
- [43] Waigh T A, Gidley M J, Komanshek B U, et al. The phase transformations in starch during gelatinisation: A liquid crystalline approach[J]. Carbohydrate Research, 2000, 328(2): 165—176.
- [44] Bertoft E. Composition of clusters and their arrangement in potato amylopectin[J]. Carbohydrate Polymers, 2007, 68(3): 433—446.
- [45] Bertoft E. On the nature of categories of chains in amylopectin and their connection to the super helix model[J]. Carbohydrate Polymers, 2004, 57(2): 211—224.
- [46] 赵米雪, 包亚莉, 刘培玲. 淀粉颗粒微观精细结构研究进展[J]. 食品科学, 2018, 39(11): 284—294.
Zhao Mixue, Bao Yali, Liu Peiling. Progress in research on fine microstructure of starch granules[J]. Food science, 2018, 39(11): 284—294. (in Chinese with English abstract)

Separation effect of sweet potato amylose and amylopectin with different chain length by artificial zeolite

Guo Junjie¹, Yang Lu¹, Fu Fangfang¹, Lian Xijun^{1*}, Wang Xueqing¹, Kang Haiqi²

(1. Tianjin Key Laboratory of Food Biotechnology, School of Biotechnology and Food Science, Tianjin University of Commerce, Tianjin 300134, China;

2. Crops Research Institute, Sichuan Academy of Agricultural Science, Chengdu 610066, China)

Abstract: Column chromatography is based on the difference of physicochemical properties of components in the mixture. The mixture is separated after multiple distributions by using the different distribution coefficients of each component in the stationary and mobile phase. The starch was hydrolyzed by amylase after retrogradation under high pressure and humidity. Then, the retrograde starch was dissolved by 4 mol/L potassium hydroxide and the solution was adjusted to neutral next. The precipitate of amylose was obtained by adding n-butanol to the solution. While, amylopectin was prepared by adding ethanol to the supernatant. Both of amylose and amylopectin in sweet potato were retrograded for the second time to narrow their molecular weight distribution. And column chromatography was used to separate the components furtherly. The total yields of amylose and amylopectin were more than 2.4% respectively. The results of visible spectrum and molecular weight distribution showed that M_w of amylose and amylopectin narrowed to 1641-2069 g/mol and 1671-2167 g/mol, respectively, while M_n narrowed to 1516-1710 g/mol and 1526-1678 g/mol. The corresponding PDI of amylose ranged from 1.082-1.209, and PDI of amylopectin ranged from 1.095-1.291. Artificial zeolite with 1-3 mm diameter was suitable for the separation of amylopectin, while artificial zeolite with 4-6 mm diameter was suitable for amylose. In the course of separation, amylose with higher DP adsorbed on the macrozeolite surface. It was eluted out from the mixture first for the weaker adsorption force. Amylose with lower DP entered into the small holes of macrozeolite, and was eluted out subsequently for the stronger adsorption force. When separated by small zeolite column chromatography, the amylopectin components of F1b with small molecular weight and high homogeneity were eluted out first. While, amylopectin components of F2b with large molecular weight and low homogeneity were eluted out first, indicating that the branching degree of amylopectin also played a certain role in the separation of starch components by zeolite column chromatography. X-ray diffraction showed distinctive spectra. Amylose components revealed strong sharp peaks at the diffraction angles (2θ) of 18.9°, 23.4°, 27.2°, 29.3°, 32.3°, 33.7°. Amylopectin components showed obvious sharp peaks at around 21.6°, 22.9°, 23.9°, 26.5°, 27.1°, 29.3°, 34.1°, 35.8°, 39.5°. The molecular weight distribution index (PDI) of sweet potato amylose was close to 1.0 at the same time. Amylose and amylopectin with extreme narrow molecular weight exhibited sharp peaks like metallic salts. That could be used for the study of the spatial structure changes of starch macromolecules in depth. Micrographs showed that amylose was composed of many linear molecules and presented typical linear “wicker-like” morphology, while amylopectin showed “branch-like” shape. The results provide a simple and efficient method for the preparing of amylose and amylopectin with extreme narrow molecular weight distribution. It brings about favorable conditions for further exploring morphological changes of starch macromolecules during aggregation progress.

Keywords: enzyme; strach; zeolite; column chromatography; separation